

AperTO - Archivio Istituzionale Open Access dell'Università di Torino

Emergence of multiple EGFR extracellular mutations during cetuximab treatment in colorectal cancer

This is the author's manuscript

Original Citation:

Availability:

This version is available <http://hdl.handle.net/2318/1508090> since 2017-05-17T16:42:06Z

Published version:

DOI:10.1158/1078-0432.CCR-14-2821

Terms of use:

Open Access

Anyone can freely access the full text of works made available as "Open Access". Works made available under a Creative Commons license can be used according to the terms and conditions of said license. Use of all other works requires consent of the right holder (author or publisher) if not exempted from copyright protection by the applicable law.

(Article begins on next page)



UNIVERSITÀ DEGLI STUDI DI TORINO

This is an author version of the contribution published on:

Questa è la versione dell'autore dell'opera:

Arena S, Bellosillo B, Siravegna G, Martínez A, Cañadas I, Lazzari L, Ferruz N, Russo M, Misale S, González I, Iglesias M, Gavilan E, Corti G, Hobor S, Crisafulli G, Salido M, Sánchez J, Dalmases A, Bellmunt J, De Fabritiis G, Rovira A, Di Nicolantonio F, Albanell J, Bardelli A, Montagut C. Emergence of Multiple EGFR Extracellular Mutations during Cetuximab Treatment in Colorectal Cancer. Clin Cancer Res. 2015 May 1;21(9):2157-66. Epub 2015 Jan 26.

doi: 10.1158/1078-0432.CCR-14-2821

The definitive version is available at:

La versione definitiva è disponibile alla URL:

<http://clincancerres.aacrjournals.org/content/21/9/2157.long>

Emergence of multiple EGFR extracellular mutations during cetuximab treatment in colorectal cancer

Sabrina Arena^{* 1,4,5}, Beatriz Bellosillo^{* 2,3}, Giulia Siravegna^{1,4}, Alejandro Martínez^{2,6}, Israel Cañadas², Luca Lazzari^{1,4}, Noelia Ferruz⁷, Mariangela Russo^{1,4}, Sandra Misale¹, Iria González⁶, Mar Iglesias³, Elena Gavilan², Giorgio Corti¹, Sebastijan Hobor^{1,#}, Giovanni Crisafulli¹, Marta Salido³, Juan Sánchez⁸, Alba Dalmases^{2,3}, Joaquim Bellmunt², Gianni De Fabritiis^{7,9}, Ana Rovira², Federica Di Nicolantonio^{1,4}, Joan Albanell^{2,6,10}, Alberto Bardelli^{§,1,4}, Clara Montagut^{§ 2,6}

Affiliations: ¹Candiolo Cancer Institute-FPO, IRCCS, Candiolo, Italy; ²Cancer Research Program, FIMIM, Hospital del Mar, Barcelona, Spain; ³Pathology Department, Hospital del Mar, Barcelona, Spain; ⁴University of Torino, Department of Oncology, Candiolo, Italy; ⁵FIRC Institute of Molecular Oncology (IFOM), Milano, Italy; ⁶Medical Oncology Department, Hospital del Mar, Barcelona, Spain; ⁷Computational Biophysics Laboratory (GRIB-IMIM), Pompeu Fabra University, PRBB, Barcelona, Spain; ⁸Radiology Department, Hospital del Mar, Barcelona, Spain; ⁹Institució Catalana de Recerca i Estudis Avançats, Barcelona, Spain; ¹⁰Pompeu Fabra University, Barcelona, Spain.

Running title: EGFR mutations and resistance to cetuximab

Keywords: Colorectal neoplasms, GI neoplasms, EGFR, resistance, cetuximab

Financial support: This work was supported by RD12/0036/0051, PI12/00989, PI12/00680, PT13/0010/0005, 2014 SGR 567 and 2014 SGR 740 grants and by the Xarxa de Banc de Tumors de Catalunya (C.M.). The European Community's Seventh Framework Programme under grant agreement no. 259015 COLTHERES (A.B.); Associazione Italiana per la Ricerca sul Cancro (AIRC) IG grant no. 12812 (A.B.); AIRC MFAG no. 11349 (F.D.N.); grant —Farmacogenomicall—5 per mille 2009 MIUR—Fondazione Piemontese per la Ricerca sul Cancro—ONLUS (F.D.N.); AIRC 2010 Special Program Molecular Clinical Oncology 5 per mille, project no. 9970 (A.B.); FPRC 5 per mille 2010 and 2011

Ministero della Salute (A.B.); Ministero dell'Istruzione, dell'Università e della Ricerca, progetto PRIN 2010-2011 (A.B.). J.A. is a recipient of intensification program ISCIII/FEDER. We thank Fundació Cellex (Barcelona) for a generous donation to the Hospital del Mar Medical Oncology Service.

Potential Conflicts of Interest: None to Disclose

* co-first authors

#present address: Cancer Research UK London Research Institute, London

§ co-senior authors

Correspondence to:

Alberto Bardelli, University of Torino, Department of Oncology, Str prov 142 Km 3.95, 10060 Candiolo, Torino, Italy. Telephone: +39 011 9933235; e-mail address: alberto.bardelli@unito.it and **Clara Montagut**, Medical Oncology Department, Hospital del Mar, Passeig Maritim 25-29, Barcelona 08003, Spain. Telephone: + 34 93 248 3137; e-mail address: cmontagut@hospitaldelmar.cat

Word Count: 4190 words

Figures: 2 Tables and 3 figures

Supplementary Figures: 3 supplementary tables and 3 supplementary figures

Statement of translational relevance

The anti-EGFR monoclonal antibody cetuximab is effective for the treatment of patients with 'RAS' wild-type metastatic colorectal cancer (mCRC). Unfortunately, responses are transient and most patients develop acquired resistance. In the present study, we analysed the genetic profile of clinical specimens and preclinical models of acquired resistance to cetuximab, revealing a complex pattern of mutations in both EGFR and its downstream effectors, KRAS, NRAS, BRAF and PIK3CA. We discovered five novel point mutations in the ectodomain of EGFR, which confer resistance to cetuximab. Of note, only a subset of these EGFR variants remains sensitive to panitumumab. Accordingly, identification patient-specific mechanisms of resistance to EGFR blockade will be paramount to design additional lines of therapy.

Abstract

Purpose: Colorectal cancer (CRC) patients who respond to the anti-EGFR antibody cetuximab often develop resistance within several months of initiating therapy. To design new lines of treatment the molecular landscape of resistant tumors must be ascertained. We investigated the role of mutations in the EGFR signalling axis on the acquisition of resistance to cetuximab in patients and cellular models.

Experimental Design: Tissue samples were obtained from 37 CRC patients who became refractory to cetuximab. CRC cells sensitive to cetuximab were treated until resistant derivatives emerged. Mutational profiling of biopsies and cell lines was performed. Structural modeling and functional analyses were performed to causally associate the alleles to resistance.

Results: The genetic profile of tumor specimens obtained after cetuximab treatment revealed the emergence of a complex pattern of mutations in *EGFR*, *KRAS*, *NRAS*, *BRAF* and *PIK3CA* genes, including two novel EGFR ectodomain mutations (R451C and K467T). Mutational profiling of cetuximab resistant cells recapitulated the molecular landscape observed in clinical samples and revealed three additional *EGFR* alleles: S464L, G465R and I491M. Structurally, these mutations are located in the cetuximab-binding region, except for the R451C mutant. Functionally, *EGFR* ectodomain mutations prevent binding to cetuximab but a subset is permissive for interaction with panitumumab.

Conclusion: Colorectal tumors evade EGFR blockade by constitutive activation of downstream signalling effectors and through mutations affecting receptor-antibody binding. Both mechanisms of resistance may occur concomitantly. Our data have implications for designing additional lines of therapy for CRC patients who relapse upon treatment with anti-EGFR antibodies.

Introduction

Monoclonal antibodies (moAbs) directed against the epidermal growth factor receptor (EGFR) --cetuximab and panitumumab-- provide significant survival benefit to patients with *RAS* wild-type metastatic colorectal cancer (mCRC) and are now standard components of treatment regimens for these patients, either alone or in combination with chemotherapy. However, the duration of this response is only transient and does not last more than 3 to 12 months, after which secondary resistance occurs (1-5). Definition of the molecular changes underlying acquired resistance to anti-EGFR antibodies is needed to improve clinical benefit and devise further lines of treatment. Molecular profiling of patient samples and preclinical models have previously defined a number of mechanisms of secondary resistance. The most common event is the emergence of *KRAS* and *NRAS* mutations which occurs in approximately 50-80% of the cases (6-10). Other escape routes include acquisition of the S492R mutation in the ectodomain of EGFR (10-13), as well as amplification of tyrosine kinase receptor genes *HER2* or *MET* (14, 15). Interestingly, recent data indicate co-existence of several molecular mechanisms of secondary resistance within an individual patient (6-10, 12, 16).

To identify yet unknown molecular events leading to anti-EGFR treatment failure, we investigated the role of mutations in the EGFR signaling pathway on the acquisition of resistance to cetuximab in CRC patients and cellular models. Our findings suggest that we have yet to fully characterize the complete spectrum of genetic variants through which colorectal tumors evade EGFR blockade. The data presented here will help design additional therapeutic strategies to circumvent resistance of CRC patients who receive EGFR targeted antibodies.

Materials and Methods

Tumor samples and patients

All mCRC consenting patients treated with anti-EGFR moAb at Hospital del Mar between January 2010 and June 2013 were included in this study. In the analysis, we only included patients who had good quality paired pre- and post- treatment biopsies and who acquired resistance to anti-EGFR based-therapy defined as progression disease following a) complete response or partial response or b) stable disease for more than 16 weeks.

Response was evaluated according to the Response Evaluation Criteria in Solid Tumors (RECIST) (17). Our study included re-biopsy following treatment failure in patients who consented to this extra procedure. Re-biopsies at the time of progression were obtained from the most accessible lesion with less potential risk of related complications for the patient according to ethical considerations. Pre-treatment sample was obtained from the regular diagnosis procedure. In this study, we included nine cases (patients #21 to #28 and patient #36) that had been previously assessed for *EGFR* S492R, *KRAS* exon 2, *BRAF* V600E and *PIK3CA* mutations by Sanger sequencing (12) and that in the current work were analyzed for a broader panel of mutations as specified below using more sensitive sequencing technologies. Biological samples were obtained from Parc de Salut Mar Biobank (MARBiobanc). This study was approved by the local Ethics Board (CEIC-2012/4741/I). All participating patients signed written informed consent.

Mutational analysis in tissue samples

DNA extraction from tumoral samples was performed as previously described (12). Mutational analysis of *KRAS* (exons 2, 3 and 4), *BRAF* (exon15), *NRAS* (exons 2 and 3), *PIK3CA* (exons 9 and 20) and *EGFR* (exon 12) was performed by Sanger sequencing using BigDye v3.1 (Applied Biosystems, Foster City, CA) following manufacturer's instructions and analyzed on a 3500Dx Genetic Analyzer (Applied Biosystems). *KRAS* (exons 3 and 4) and *NRAS* (exons 2, 3 and 4) were also analyzed by pyrosequencing (Qiagen) and *KRAS* (exon 2) was also assessed by Therascreen real time PCR (Qiagen) following the manufacturer's instructions. All cases were also screened by pyrosequencing using a Next Generation Sequencing (NGS) 454 GS Junior platform (Roche Applied Science, Mannheim, Germany). Processed and quality-filtered reads were analyzed using the GS Amplicon Variant Analyzer software version 2.5p1 (Roche). Mutations detected by NGS were confirmed by competitive allele-specific TaqMan® PCR (CAST-PCR, Applied Biosystems) when specific assays were available.

Cell culture and generation of resistant cells

DiFi cells were cultured in F12 medium (Invitrogen) supplemented with 5% FBS; OXCO-2 cells were cultured in Iscove's medium (Invitrogen) supplemented with 5% FBS; LIM1215 cells were cultured in RPMI-1640 medium (Invitrogen) supplemented with 5% FBS and insulin (1 µg/ml); NCIH508 cells were cultured in RPMI-1640 medium (Invitrogen) supplemented with 5% FBS; HCA-46 cells were cultured in DMEM medium (Invitrogen)

supplemented with 5% FBS and CCK81 cells were cultured in MEM medium (Invitrogen) supplemented with 5% FBS. All media contained also 2mM L-glutamine, antibiotics (100U/mL penicillin and 100 mg/mL streptomycin) and cells were grown in a 37°C and 5% CO₂ air incubator. The DiFi and OXCO-2 cell lines were a kind gift from Dr. J. Baselga in November 2004 (Oncology Department of Vall d'Hebron University Hospital, Barcelona, Spain) and Dr V. Cerundolo in March 2010 (Weatherall Institute of Molecular Medicine, University of Oxford, UK), respectively. The LIM1215 parental cell line has been described previously (18) and was obtained from Prof. Robert Whitehead, Vanderbilt University, Nashville, with permission from the Ludwig Institute for Cancer Research, Zurich, Switzerland. The NCIH508 cell line was purchased from American Type Culture Collection (LGC Standards S.r.l). HCA-46 cell lines was obtained from ECACC (distributed by Sigma-Aldrich Srl). CCK81 cell line was obtained from HSRRB, Japan. The identity of each cell line was tested and authenticated by Cell ID™ System and by Gene Print® 10 System (Promega), through Short Tandem Repeats (STR) at 10 different loci (D5S818, D13S317, D7S820, D16S539, D21S11, vWA, TH01, TPOX, CSF1PO and amelogenin). Amplicons from multiplex PCRs were separated by capillary electrophoresis (3730 DNA Analyzer, Applied Biosystems) and analyzed using GeneMapperID software from Life Technologies. Resulting cell line STR profiles were cross-compared and matched with the available STR from ATC, ECCAC, and CellBank Australia repositories online databases. All cell lines were tested and resulted negative for mycoplasma contamination with Venor® GeM Classic kit (Minerva biolabs).

Generation of resistant cells utilized in this manuscript has already been previously described (6, 9). CCK81 cetuximab-resistant derivatives were obtained by increasing the cetuximab dosage stepwise from 680 nM to 1.4 µM during the course of six months.

Mutational analysis in cell lines

Genomic DNA samples were extracted by Wizard® SV Genomic DNA Purification System (Promega). For Sanger Sequencing, all samples were subjected to automated sequencing by ABI PRISM 3730 (Applied Biosystems). Primer sequences are listed elsewhere (6, 9). The following genes and exons were analyzed: *KRAS* (exons 2, 3 and 4), *NRAS* (exons 2 and 3), *PIK3CA* (exons 9 and 20), *BRAF* (exon 15), *EGFR* (exon12). All mutations were confirmed twice, starting from independent PCR reactions.

Drug assays

Cetuximab was obtained from the Pharmacy at Niguarda Ca' Granda Hospital, Milan, Italy. Cell lines were seeded in 100 μL medium at the following densities (2×10^3 for DiFi, 1.5×10^3 for LIM1215, HCA-46, NCIH508 and OXCO-2, 3×10^3 for CCK81) in 96-well culture plates. After serial dilutions, cetuximab in serum-free medium was added to cells, and medium-only wells were included as controls. Plates were incubated at 37°C in 5% CO_2 for 6 days, after which cell viability was assessed by ATP content using the CellTiter-Glo® Luminescent Assay (Promega).

DNA constructs and mutagenesis

The pLX301-EGFR WT construct was a generous gift from Dr. C. Sun and Prof R. Bernards (NKI, Amsterdam). *EGFR* mutants containing the 6 point mutations (R451C, S464L, G465R, K467T, I491M and S492R) were constructed using the QuikChange® II site-directed mutagenesis kits from Agilent Technologies with pLX301-EGFR WT plasmid as the template DNA. The presence of mutations was confirmed by DNA sequencing.

Droplet Digital PCR

Isolated gDNA was amplified using ddPCR™ Supermix for Probes (Bio-Rad) using *KRAS*, *NRAS*, *BRAF* and *EGFR* assay (PrimePCR™ ddPCR™ Mutation Assay, Bio-Rad and custom designed). ddPCR was performed according to manufacturer's protocol and the results reported as percentage or fractional abundance of mutant DNA alleles to total (mutant plus wild type) DNA alleles. 8 to 10 μL of DNA template was added to 10 μL of ddPCR™ Supermix for Probes (Bio-Rad) and 2 μL of the primer/probe mixture. This 20 μL sample was added to 70 μL of Droplet Generation Oil for Probes (Bio-Rad) and used for droplet generation. Droplets were then thermal cycled with the following conditions: 5 minutes at 95°C , 40 cycles of 94°C for 30s, 55°C for 1 minute followed by 98°C for 10 minutes (Ramp Rate $2^\circ\text{C}/\text{sec}$). Samples were then transferred to a QX200™ Droplet Reader (Bio-Rad) for fluorescent measurement of FAM and HEX probes. Gating was performed based on positive and negative controls, and mutant populations were identified. Fractional Abundances of the mutant DNA in the wild-type DNA background were calculated for each sample using QuantaSoft software (Bio-Rad). Multiple replicates (minimum of four) were performed for each sample. ddPCR analysis of normal control gDNA from cell lines and no DNA template (water) controls were performed in parallel with all the samples, including again multiple replicates as a contamination-free control.

EGFR probes and primers sequences are available upon request.

Molecular Simulations

Input coordinates for the structure of cetuximab bound to wild type sEGFR (extracellular part) were taken from PDB:1YY9 (19). The system was parameterized using the Amber12 force field (20) and solvated and neutralized in a TIP3P water box. Energy minimization was conducted under NPT conditions at 1 atm, 298K and a cutoff of 9 Å, with rigid bonds and PME for long-range electrostatics. Potential energy minimization was run for 2ps. During minimization the heavy protein atoms were not restrained. The simulation was run using ACEMD (21) on a local GPU-equipped workstation.

Flow Cytometry

To measure cetuximab and panitumumab binding to cells expressing mutant EGFR, we harvested by trypsinization and washed the cells twice with PBS. We incubated the cells with Fc blocking solution for 15 m on ice to block non-specific Fc binding of immunoglobulins. We then washed the cells and incubated them with the monoclonal antibodies for EGFR binding during 30 m on ice. To visualize the primary antibody a goat anti-human IgGγ ficoerythrin-conjugated (Invitrogen) was used as a secondary antibody. EGFR binding was analyzed using the FACScan flow Cytometer.

Protein detection

We subjected total cell lysates to Western blot analysis as previously reported (12). The phospho EGFR antibody (Y1068) was purchased from Cell Signalling Technology.

Results

Emergence of EGFR ectodomain mutations in patients treated with cetuximab

Thirty-seven consecutive patients with metastatic colorectal cancer who had acquired resistance to cetuximab after an initial response to the treatment and had good quality paired pre- and post- treatment specimens were included in this study. Tumor biopsy obtained during the regular diagnosis procedure was used as the pre-treatment sample. In most cases this sample was obtained from the primary tumor during routine colonoscopy. Biopsies at progression were taken from liver (21 samples), lung (6), bone (2), peritoneum (3), colon-rectum (3), retroperitoneal lymph node (1) and subcutaneous node (1) with

ultrasound guidance, CT-scan guidance, or colonoscopy in the case of colon-rectum lesions. There were no major biopsy-related complications. Patients' clinical characteristics are showed in Supplementary Table S1.

All pre-treatment biopsies were screened for mutations in *KRAS*, *NRAS* and *BRAF* by Sanger and pyrosequencing as part of routine clinical practice at Hospital del Mar (Barcelona). Mutations in *PIK3CA* and *EGFR* were also assessed as part of this study. All pre-treatment biopsies were wild type except for three samples that harbored mutations in *PIK3CA*. Since *PIK3CA* mutations do not preclude response to anti-EGFR therapy, these patients were treated with cetuximab-based regimens. Post-treatment tissue samples were analyzed for the same mutations using the same sequencing platforms. In total, we detected the emergence of 31 mutations in post-treatment biopsies from 20 patients (Table 1). The additional 17 post treatment samples did not reveal variants in any of the genes we analyzed. In seven cases, mutations in different genes were detected in the same tissue sample (median of detected mutations within the same specimen 2, range 1-5) (Table 1).

Acquired mutations were found in *NRAS* (9 events) and *KRAS* genes (8 events) followed by mutations in *PIK3CA* (6 events) and *BRAF* (3 events). Interestingly, mutations in *RAS* frequently occurred in exons 3-4 (67% of *NRAS* and 50% of *KRAS* mutations). Of note, mutations in *PIK3CA* always coexisted with other mutations within the same sample.

Notably, in addition to 'RAS' gene mutations the molecular analysis revealed the emergence of multiple alleles in the EGFR extracellular domain. The previously reported *EGFR S492R* variant was detected in three patients. Of note, *EGFR* mutations were accompanied by gene amplification in both the pre- and the post- treatment specimen from two of these patients (data not shown); in the third patient, EGFR gene copy number was not assessed due to lack of sufficient tissue for FISH analysis.

Two novel mutations located in exon 12 of the *EGFR* gene were discovered by the analysis of post treatment samples. Patient #31 harboured an A -> C substitution at codon 1400 that caused a substitution of a lysine to threonine at aminoacid 467 (p.K467T). The post-cetuximab biopsy from patient #35 harbored a C -> A substitution at codon 1351,

resulting in an arginine to cysteine substitution at aminoacid 451 (p.R451C) (Table 1 and Supplementary Fig. S1).

EGFR ectodomain mutations and acquired resistance to cetuximab in CRC cell models

We previously reported that acquisition of resistance in CRC cells is associated with emergence of *KRAS*, *BRAF* and *NRAS* activating mutations (6, 9, 12). To discover additional mechanisms of resistance to EGFR blockade we exploited 5 CRC cell lines (DiFi, LIM1215, HCA-46, NCIH508, OXCO-2 and CCK81), which are highly sensitive to cetuximab (Supplementary Fig. S2). These cell lines are wild type for *KRAS*, *NRAS*, *BRAF* and *PIK3CA* with the exception of NCIH508, which displays the p.E545K *PIK3CA* mutation. Altogether, these cell models recapitulate the molecular features of tumors from CRC patients likely to respond to anti EGFR therapies. For each line, at least five million cells were exposed continuously to cetuximab until resistant populations emerged (Supplementary Fig. S2). To define molecular mechanisms underlying acquisition of resistance, we initially performed Sanger sequencing of genes involved in regulation of the EGFR signalling pathway (*EGFR*, *KRAS*, *BRAF*, *NRAS*, and *PIK3CA*). In accordance with our previous reports, resistant populations often displayed *KRAS*, *BRAF* and *NRAS* mutations (Table 2) (9). All of these alleles were detected in the resistant cells but not in the corresponding parental population from which they originated. Importantly, in several occasions multiple genetic alterations were concomitantly present in the resistant cell population (Table 2) indicating their polyclonal status. To assess the molecular features of individual clones we performed limited cell dilutions of LIM1215 and CCK81 as these cell lines are amenable to this procedure. We then subjected single clones to Sanger sequencing for candidate genes (*EGFR*, *KRAS*, *BRAF*, *NRAS*, and *PIK3CA*). Notably, mutation profiling of clones identified three novel *EGFR* variants: S464L, G465R and I491M (Supplementary Fig. S3). Considering that the resistant derivatives are polyclonal, and in light of the limited sensitivity of the Sanger sequencing method, we postulated that variants present in less than 20% of the cell populations might have remained undetected. To identify mutations present at low frequency we employed droplet digital PCR (ddPCR) which is known to have a mutant/wild type sensitivity of 1:20000. ddPCR probes were designed and individually validated using control mutant DNA to detect *EGFR* variants previously identified in tumor biopsy or cell lines (Supplementary Table S2). This analysis unveiled the presence 3 new *EGFR* variants (S464L, G465R, and I491M) that were not detected by Sanger sequencing in resistant cell populations (Table 2 and Supplementary

Table S3). The ddPCR approach could not be performed in tissue samples since there was no sufficient material available. Overall, the mutational landscape of cell lines with acquired resistance to cetuximab, recapitulate the molecular profiles of tumors that relapsed upon cetuximab treatment.

Structural model analysis of EGFR ectodomain mutations

To understand how the EGFR ectodomain mutations detected in tumor samples and cell lines could drive resistance to EGFR blockade we performed computational structure-based analyses. With the exception of R451C, the EGFR mutations are located in the receptor region, which has been shown to interact with cetuximab (Fig. 1A). More specifically, the S464L, G465R, K467T, I491M and S492R mutations lie in the middle of the surface recognized by the antibody (Fig. 1B) and therefore modifications of this interface has the potential to affect complex formation. Of these five mutations, three appear to disrupt favourable interactions, namely S464L, K467T, and I491M. The polar aminoacid S464 is within H-bond distance from the carbonyl backbone of Y102 and the phenolic OH-group of Y104 (Fig. 1C). Replacement by a hydrophobic bulky aminoacid as leucine (S464L) has the potential to disrupt the network. Analogously, the positively charged aminoacid K467 is involved in a stabilizing salt bridge with E58 (Fig. 1C). Insertion of a polar but neutral aminoacid as threonine K467T, although still permitting the H-bond E58, would affect the favourable electrostatic interaction. Residue I491 is a rather large, aliphatic residue located in a hydrophobic cavity mainly formed by aromatic aminoacids (Fig. 1C). Although the side chains present similar size, methionine (I491M) is a polar aminoacid and would be unfavourably located in a nonpolar environment. The other two mutations (G465R and S492R) involve the change from rather small, polar and uncharged side chain to a large and electrically charged side chain in arginine (Fig. 1C) (13).

R451C is the only mutation not located in the cetuximab-binding site, however, the mutation could lead to critical structural changes. As the domain IV is formed by a sequence of disulphide bonds, which preserve its tertiary structure, the replacement by a cysteine at that position could perturb one of the disulphide bonds in domain III (C475-C462) possibly forming a new one between domains III and IV (C451-C475). We verified that the distance in the crystal structure between these residues (C451-C475, carbon alpha distance 6.8 Å) is compatible with the formation of a disulphide bond. Indeed, a system setup in this new configuration successfully minimizes to a C451-C475 distance of

5.2 Å. Overall, all identified mutations in EGFR (except R451C) were located in the cetuximab binding epitope.

Biochemical and functional analyses of EGFR ectodomain mutations

To experimentally assess the impact of the EGFR ectodomain mutations on the ability of the receptor to interact with cetuximab we performed forward genetic experiments on a subset of the newly discovered mutations. Wild type and mutant *EGFR* cDNAs were ectopically expressed in NIH 3T3 cells that lack endogenous EGFR. Flow cytometry was used to establish the extent of cetuximab binding to cells expressing the mutants; wild type *EGFR* and *S492R* served as positive and negative controls respectively. These experiments clearly showed that the newly discovered EGFR K467T, R451C, S464L, G465R and I491M mutations were not permissive for binding to cetuximab thus providing functional evidence of their role in driving acquired resistance to EGFR blockade. Of note, the effect of *EGFR* R451C on cetuximab binding was less prominent compared to the other mutants (Fig. 2).

To further characterize the functional properties of the EGFR mutations we performed biochemical studies in cells expressing individual mutations. As expected cetuximab abrogated ligand-mediated activation of the wild type receptor, while had no or very limited impact in cells carrying mutated EGFR (S464L, G465R, K467T, I491M and S492R) (Fig. 3). Notably, in R451C mutant cells, cetuximab was still capable of inhibiting EGFR phosphorylation (Fig. 3).

We then examined whether panitumumab, the other anti-EGFR drug approved to treat CRC, was active in cells overexpressing EGFR mutations. As previously described, S492R mutant cells efficiently bound to panitumumab (12). We found that the K467T and R451C mutants were to some extent permissive for panitumumab binding, while S464L, G465R and I491M mutants did not bind to this antibody (Fig. 2). Accordingly, biochemical analyses showed that panitumumab prevents EGFR activation in S492R, K467 and R451C mutants (Fig. 3).

Discussion

We present a comprehensive analysis of mutational changes affecting key members of the EGFR signaling pathway emerging in tumor biopsies of patients treated with cetuximab and in cell models, which acquired resistance to cetuximab *in vitro*. We found that colorectal cancer cells evade EGFR blockade through two main strategies. The main mechanism of resistance involves downstream pathway reactivation which occurs in 43% of patients' samples and 58.8% of the cells respectively. The second entails EGFR extracellular domain mutations that were we detected in 10.8% of patients' samples and 29% of the cells. Although these different codons in cells and patients, our findings highlights a remarkable overlap among the resistant mechanism observed in preclinical models and patients samples (22). The cell-based findings may be translated back into the clinic. For example the EGFR ectodomain alleles, initially discovered in cells, might reasonably also be present in patients who relapse upon EGFR blockade and this could be verified using tissue and liquid biopsies.

The molecular landscape of acquired resistance to EGFR blockade revealed the emergence of multiple point mutations in the ectodomain of EGFR. In particular we detected two novel EGFR exon 12 mutations (EGFR p.R451C and p.K467T) in two patients. The previously reported *EGFR* S492R mutation was detected in 3 out of 37 post-cetuximab tissue samples (8%), while a recent study reports 16% of S492R EGFR mutation detection in 239 post-cetuximab plasma samples (11). Such differences may be explained by different sensitivity of the detection techniques as well as the ability of plasma samples to capture the heterogeneity of solid tumors as compared to single biopsies of one tumoral lesion (8, 16, 23). Plasma samples of the patients included in the current study were not systematically collected and therefore we could not analyze the prevalence of EGFR mutations in circulating tumor DNA in the cohort. Accordingly, studies in larger cohorts of patients treated with cetuximab or panitumumab are warranted to define the exact frequency of the other newly identified EGFR ectodomain mutations. Of note, most samples harboring the *EGFR* S492R mutation also exhibited *EGFR* gene amplification (12), similar to lung cancer tumors harboring the T790M mutation of resistance to tyrosine-kinase inhibitors, where the T790M allele appears to be selectively amplified (24). Interestingly, our *in vitro* analysis showed that panitumumab was effective in a subset of EGFR mutants. Since the binding epitopes of cetuximab and panitumumab overlap but are

not identical, it is foreseeable that mutations arising in EGFR after anti-EGFR treatment will differentially disrupt binding of cetuximab and/or panitumumab to the receptor (25), with relevant clinical implications for the treatment of cetuximab resistant patients.

Activating mutations in EGFR downstream signaling effectors were the most frequent event in both cell models and patients. Emergence of *KRAS* and *NRAS* mutations occurred in 42% of patients, similar to what we have previously reported in tissue samples, but lower than previously reported in plasma samples (6-10). Again, this may be due to the advantage of circulating DNA in capturing the heterogeneity of solid tumors compared to biopsy of one tumoral lesion (8, 16, 23), indicating that diagnostic tools such as liquid biopsies are required to capture the complexity of the disease. As recently reported, RAS mutations often occurred outside of exon 2 in clinical samples and cell models (26, 27). The finding that codon 61 and 146 *KRAS* mutations occur more frequently in the acquired resistance setting than in the general colorectal cancer population is worth further studies. Of note, all samples harboring a *PIK3CA* mutation also displayed other mechanisms of resistance. The role of *PIK3CA* mutations in driving acquired, as well as primary, resistance remains controversial and needs to be further characterized. We did not identify emergence of molecular alterations in 20% of patients, suggesting limitations in the sensitivity of the detection technique, tumor heterogeneity, as well as other mechanisms of resistance such as ligand overexpression or c-MET amplification (15, 28, 29).

Importantly, multiple mechanisms of resistance were often present in the samples from relapsed tumors often displayed more than one molecular alteration. This was also observed in cell lines resistant to cetuximab, strongly suggesting their polyclonal status. This likely reflects the heterogeneity of colorectal cancers and supports the role of circulating DNA to comprehensively characterize the molecular landscape of resistance to EGFR blockade in patients. Activation of EGFR-RAS signaling axis as well as EGFR ectodomain mutations frequently co-occurred. These findings suggest the design of clinical trials that include concomitant inhibition of EGFR downstream signaling together with direct inhibition of the EGFR receptor. Considering that panitumumab seems to be ineffective on a subset of the newly discovered mutations, drugs inhibiting EGFR through different mechanism will also be needed.

Our results have implications for the care of patients as they support the necessity of re-assessing the molecular landscape of tumors after progression to anti-EGFR drugs, which currently is not routinely done in clinical practice. The plasticity of tumor cells and their high capacity of adaptation under selective drug pressure, emphasizes the need for sequential tumor or plasma biopsies to better monitor and personalize treatment.

In summary, our study highlights the importance of reassessing the molecular profile of the overall disease burden longitudinally during therapy, and provides evidence that acquired resistance to anti-EGFR therapy in mCRC patients arises from the emergence of heterogeneous and overlapping molecular changes. Such complexity converges on two main mechanisms of resistance: activating mutation in EGFR downstream signalling and mutations in EGFR ectodomain that disrupt antibody-receptor binding. In light of these findings, pharmacological studies combining inhibition of both EGFR and EGFR downstream signaling effectors to bypass cetuximab resistance are warranted.

Acknowledgements

We thank Dr. Salvatore Siena, Dr Andrea Sartore Bianchi and members of the laboratory of Molecular Genetics for critical reading and editing of this manuscript.

References

1. Karapetis CS, Khambata-Ford S, Jonker DJ, O'Callaghan CJ, Tu D, Tebbutt NC, et al. K-ras mutations and benefit from cetuximab in advanced colorectal cancer. *N Engl J Med*. 2008;359:1757-65.
2. Amado RG, Wolf M, Peeters M, Van Cutsem E, Siena S, Freeman DJ, et al. Wild-type KRAS is required for panitumumab efficacy in patients with metastatic colorectal cancer. *J Clin Oncol*. 2008;26:1626-34.
3. Van Cutsem E, Kohne CH, Hitre E, Zaluski J, Chang Chien CR, Makhson A, et al. Cetuximab and chemotherapy as initial treatment for metastatic colorectal cancer. *N Engl J Med*. 2009;360:1408-17.
4. Peeters M, Price TJ, Cervantes A, Sobrero AF, Ducreux M, Hotko Y, et al. Randomized phase III study of panitumumab with fluorouracil, leucovorin, and irinotecan (FOLFIRI) compared with FOLFIRI alone as second-line treatment in patients with metastatic colorectal cancer. *J Clin Oncol*. 2010;28:4706-13.
5. Douillard JY, Siena S, Cassidy J, Tabernero J, Burkes R, Barugel M, et al. Randomized, phase III trial of panitumumab with infusional fluorouracil, leucovorin, and oxaliplatin (FOLFOX4) versus FOLFOX4 alone as first-line treatment in patients with previously untreated metastatic colorectal cancer: the PRIME study. *J Clin Oncol*. 2010;28:4697-705.
6. Misale S, Yaeger R, Hobor S, Scala E, Janakiraman M, Liska D, et al. Emergence of KRAS mutations and acquired resistance to anti-EGFR therapy in colorectal cancer. *Nature*. 2012;486:532-6.
7. Diaz LA, Jr., Williams RT, Wu J, Kinde I, Hecht JR, Berlin J, et al. The molecular evolution of acquired resistance to targeted EGFR blockade in colorectal cancers. *Nature*. 2012;486:537-40.
8. Bettegowda C, Sausen M, Leary RJ, Kinde I, Wang Y, Agrawal N, et al. Detection of circulating tumor DNA in early- and late-stage human malignancies. *Sci Transl Med*. 2014;6:224ra24.
9. Misale S, Arena S, Lamba S, Siravegna G, Lallo A, Hobor S, et al. Blockade of EGFR and MEK intercepts heterogeneous mechanisms of acquired resistance to anti-EGFR therapies in colorectal cancer. *Sci Transl Med*. 2014;6:224ra26.
10. Morelli MP, Overman MJ, Dasari A, Kazmi SMA, Vilar Sanchez E, Eng C, et al. Heterogeneity of acquired KRAS and EGFR mutations in colorectal cancer patients treated with anti-EGFR monoclonal antibodies. *ASCO Meeting Abstracts*. 2013;31:3512.
11. Newhall K, Price T, Peeters M, Kim TW, Li J, Cascinu S, et al. Frequency of S492R mutations in the Epidermal Growth Factor Receptor: Analysis of plasma DNA from metastatic colorectal cancer patients treated with panitumumab or cetuximab monotherapy. *Annals of Oncology*. 2014;25:O-0011 ii109.
12. Montagut C, Dalmases A, Bellosillo B, Crespo M, Pairet S, Iglesias M, et al. Identification of a mutation in the extracellular domain of the Epidermal Growth Factor Receptor conferring cetuximab resistance in colorectal cancer. *Nat Med*. 2012;18:221-3.
13. Buch I, Ferruz N, De Fabritiis G. Computational modeling of an epidermal growth factor receptor single-mutation resistance to cetuximab in colorectal cancer treatment. *J Chem Inf Model*. 2013;53:3123-6.
14. Yonesaka K, Zejnullahu K, Okamoto I, Satoh T, Cappuzzo F, Souglakos J, et al. Activation of ERBB2 signaling causes resistance to the EGFR-directed therapeutic antibody cetuximab. *Sci Transl Med*. 2011;3:99ra86.
15. Bardelli A, Corso S, Bertotti A, Hobor S, Valtorta E, Siravegna G, et al. Amplification of the MET receptor drives resistance to anti-EGFR therapies in colorectal cancer. *Cancer Discov*. 2013;3:658-73.
16. Gerlinger M, Rowan AJ, Horswell S, Larkin J, Endesfelder D, Gronroos E, et al. Intratumor heterogeneity and branched evolution revealed by multiregion sequencing. *N Engl J Med*. 2012;366:883-92.

17. Eisenhauer EA, Therasse P, Bogaerts J, Schwartz LH, Sargent D, Ford R, et al. New response evaluation criteria in solid tumours: revised RECIST guideline (version 1.1). *Eur J Cancer*. 2009;45:228-47.
18. Whitehead RH, Macrae FA, St John DJ, Ma J. A colon cancer cell line (LIM1215) derived from a patient with inherited nonpolyposis colorectal cancer. *J Natl Cancer Inst*. 1985;74:759-65.
19. Li S, Schmitz KR, Jeffrey PD, Wiltzius JJ, Kussie P, Ferguson KM. Structural basis for inhibition of the epidermal growth factor receptor by cetuximab. *Cancer Cell*. 2005;7:301-11.
20. Hornak V, Abel R, Okur A, Strockbine B, Roitberg A, Simmerling C. Comparison of multiple Amber force fields and development of improved protein backbone parameters. *Proteins*. 2006;65:712-25.
21. Harvey MJ, Giupponi G, Fabritiis GD. ACEMD: Accelerating Biomolecular Dynamics in the Microsecond Time Scale. *J Chem Theory Comput*. 2009;5:1632-9.
22. Misale S, Di Nicolantonio F, Sartore-Bianchi A, Siena S, Bardelli A. Resistance to Anti-EGFR Therapy in Colorectal Cancer: From Heterogeneity to Convergent Evolution. *Cancer Discov*.
23. Diehl F, Schmidt K, Choti MA, Romans K, Goodman S, Li M, et al. Circulating mutant DNA to assess tumor dynamics. *Nat Med*. 2008;14:985-90.
24. Sequist LV, Waltman BA, Dias-Santagata D, Digumarthy S, Turke AB, Fidias P, et al. Genotypic and histological evolution of lung cancers acquiring resistance to EGFR inhibitors. *Sci Transl Med*. 2011;3:75ra26.
25. Voigt M, Braig F, Gothel M, Schulte A, Lamszus K, Bokemeyer C, et al. Functional dissection of the epidermal growth factor receptor epitopes targeted by panitumumab and cetuximab. *Neoplasia*. 2012;14:1023-31.
26. Loupakis F, Ruzzo A, Cremolini C, Vincenzi B, Salvatore L, Santini D, et al. KRAS codon 61, 146 and BRAF mutations predict resistance to cetuximab plus irinotecan in KRAS codon 12 and 13 wild-type metastatic colorectal cancer. *Br J Cancer*. 2009;101:715-21.
27. Peeters M, Oliner KS, Parker A, Siena S, Van Cutsem E, Huang J, et al. Massively parallel tumor multigene sequencing to evaluate response to panitumumab in a randomized phase III study of metastatic colorectal cancer. *Clin Cancer Res*. 2013;19:1902-12.
28. Troiani T, Napolitano S, Vitagliano D, Morgillo F, Capasso A, Sforza V, et al. Primary and acquired resistance of colorectal cancer cells to anti-EGFR antibodies converge on MEK/ERK pathway activation and can be overcome by combined MEK/EGFR inhibition. *Clin Cancer Res*. 2013;20:3775-86.
29. Hobor S, Van Emburgh BO, Crowley E, Misale S, Di Nicolantonio F, Bardelli A. TGF- α and amphiregulin paracrine network promotes resistance to EGFR blockade in colorectal cancer cells. *Clin Cancer Res*. 2014;20:6429-38.

Arena et al, Table 2. EGFR pathway mutations in parental and cetuximab resistant cell lines.

Pre-Treatment										Post-Treatment																		
Parental cell Lines	KRAS exon 2	KRAS exon 3	KRAS exon 4	NRAS exon 2	NRAS exon 3	NRAS exon 4	BRAF exon 15	PIK3CA exon 9	PIK3CA exon 20	EGFR exon 12	Resistant cell Lines	KRAS exon 2	KRAS exon 3	KRAS exon 4	NRAS exon 2	NRAS exon 3	NRAS exon 4	BRAF exon 15	PIK3CA exon 9	PIK3CA exon 20	EGFR exon 12							
																					R451C	S464L	G465R	K467T	I491M	S492R		
CCK81											CCK81 R1 Cetux																	
											CCK81 R2 Cetux																	
											CCK81 R3 Cetux																	
DiFi											DiFi R1 Cetux																	
											DiFi R2 Cetux																	
HCA-46											HCA-46 R1 Cetux																	
											HCA-46 R2 Cetux																	
LIM1215											LIM1215 R1 Cetux																	
											LIM1215 R2 Cetux																	
											LIM1215 R3 Cetux																	
											LIM1215 R4 Cetux																	
											LIM1215 R5 Cetux																	
NCIH508											NCIH508 R1 Cetux																	
											NCIH508 R2 Cetux																	
OXCO-2											OXCO-2 R1 Cetux																	
											OXCO-2 R2 Cetux																	
											OXCO-2 R3 Cetux																	

Table and Figure legends

Table 1. EGFR pathway mutations in tissue samples from metastatic colorectal cancer patients treated with cetuximab. *KRAS*, *NRAS*, *BRAF*, *PIK3CA* and *EGFR* mutations were analyzed in paired tissue samples obtained at diagnosis (pre-treatment) and at progression (post-treatment). Red boxes indicate the presence of mutations detected by clinical routine sequencing procedures.

Table 2. EGFR pathway mutations in parental and cetuximab resistant cell lines.

Parental and correspondent cetuximab resistant derivatives of DiFi, LIM1215, HCA-46, NCIH508, OXCO-2 and CCK81 cell lines were analysed for *KRAS*, *NRAS*, *BRAF*, *PIK3CA* and *EGFR* mutations. Red boxes indicate the presence of the mutations (no specified alleles); in resistant cell lines, mutational analysis for EGFR exon 12 was performed by ddPCR and red boxes indicate which EGFR ectodomain alleles emerged.

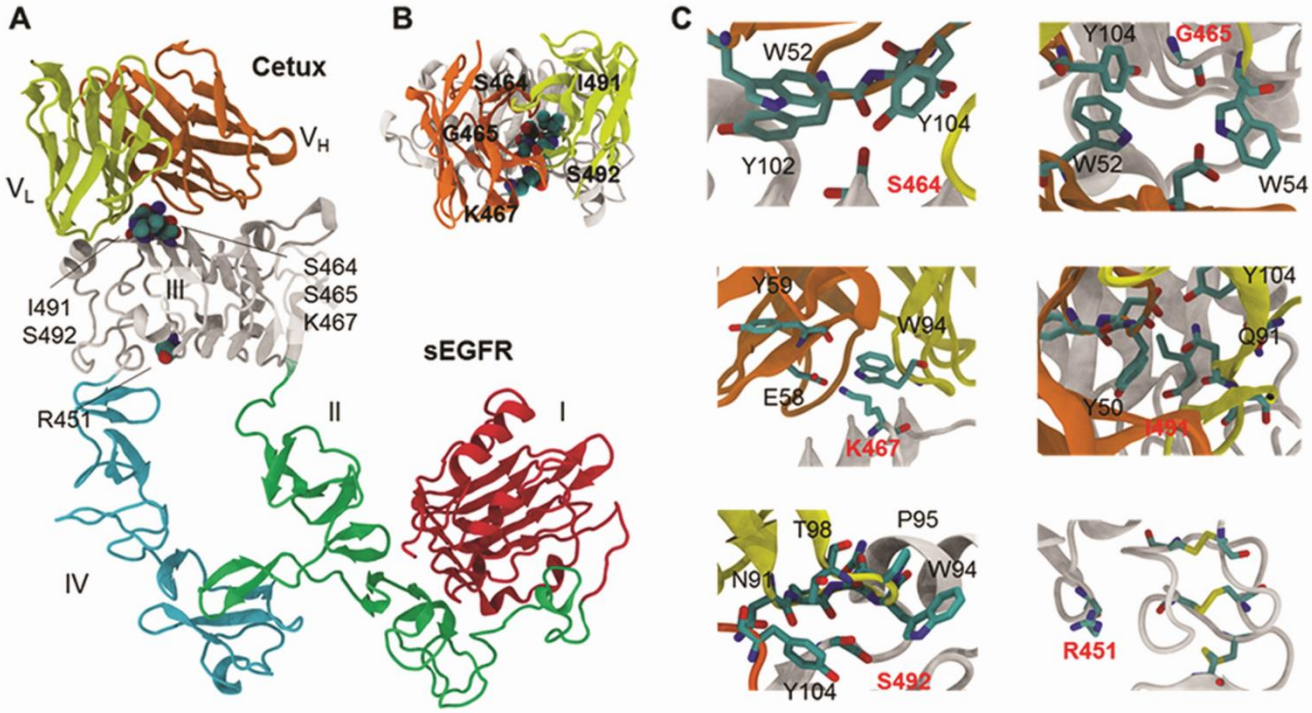
Figure 1. Structural analysis of EGFR extracellular domain mutants. A, General overview of the EGFR extracellular domain (sEGFR) bound to the antigen-binding fragment of cetuximab (Cetux) as crystallized by Li et al. Four subdomains comprise the sEGFR domain, domain III contains the six mutations. Mutation R451C occurs at the interface of contact with domain IV. B, Mutations I491M, S492R, S464L, G465R, K467T are located at the surface recognized by Cetux. A selection of residues located within 5 Å of the site of each mutation are shown. C, S464 (indicated in red, top left panel) is surrounded by Tyrosine residues (Y102 and Y104) which favor an H-bond network. G465 (indicated in red, top right panel) lies in a highly hydrophobic groove formed by Y104, W54 and W52, K467 (indicated in red, central left panel) defines a salt bridge with E58. I491 (indicated in red, central right panel) is located in a hydrophobic environment formed by Q91, Y50 and Y104. S492 (indicated in red, bottom left panel) is located in an uncharged cavity formed by Y104, W94, P95, T98 and N91. R451 (indicated in red, bottom right panel) is not located at the Cetux-sEGFR interface, but closer to the IV domain. Replacement by a Cysteine could form a new disulphide bond between domain III and IV.

Figure 2. EGFR mutations differentially affect binding to cetuximab and panitumumab. A, NIH3T3 cells stably expressing wild type or the indicated EGFR mutations were incubated with cetuximab or panitumumab, and antibody binding was

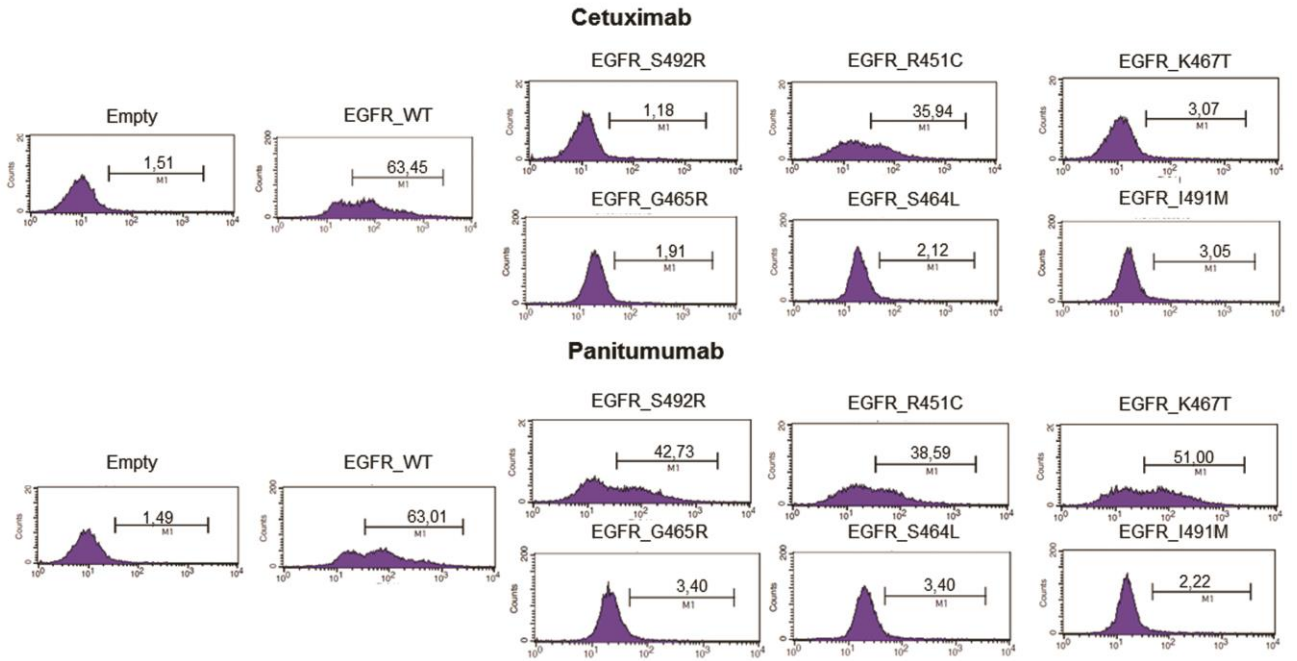
analyzed by flow cytometry using a secondary antibody to human IgG conjugated with phycoerythrin (PE). NIH 3T3 cells expressing the empty vector were used as a negative control (Empty). Graphs show results of one representative experiment. B, The percentage of cells binding to the antibody are shown as relative values compared to EGFR wild-type (wt) cells (percentage of EGFR wt cells set to 1) and are mean values of two independent experiments. While cetuximab binding was affected in cells expressing EGFR mutants, panitumumab was able to bind to cells expressing the S492R and K467T EGFR mutation. The R451C mutation had a moderate impact on binding to either cetuximab or panitumumab.

Figure 3. Ligand-dependent activation of EGFR mutants in the presence of cetuximab and panitumumab. A-G, NIH 3T3 cells expressing WT *EGFR* or the indicated *EGFR* mutations were cultured in the presence of cetuximab (Ctx) or panitumumab (Pnm) for 2 h and stimulated with EGF (5 ng/ml) for 15'. Immunoblotting was performed using antibodies to the indicated proteins.

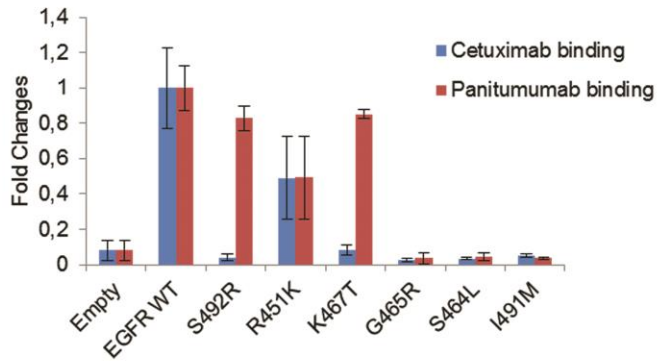
Arena et al, Figure 1



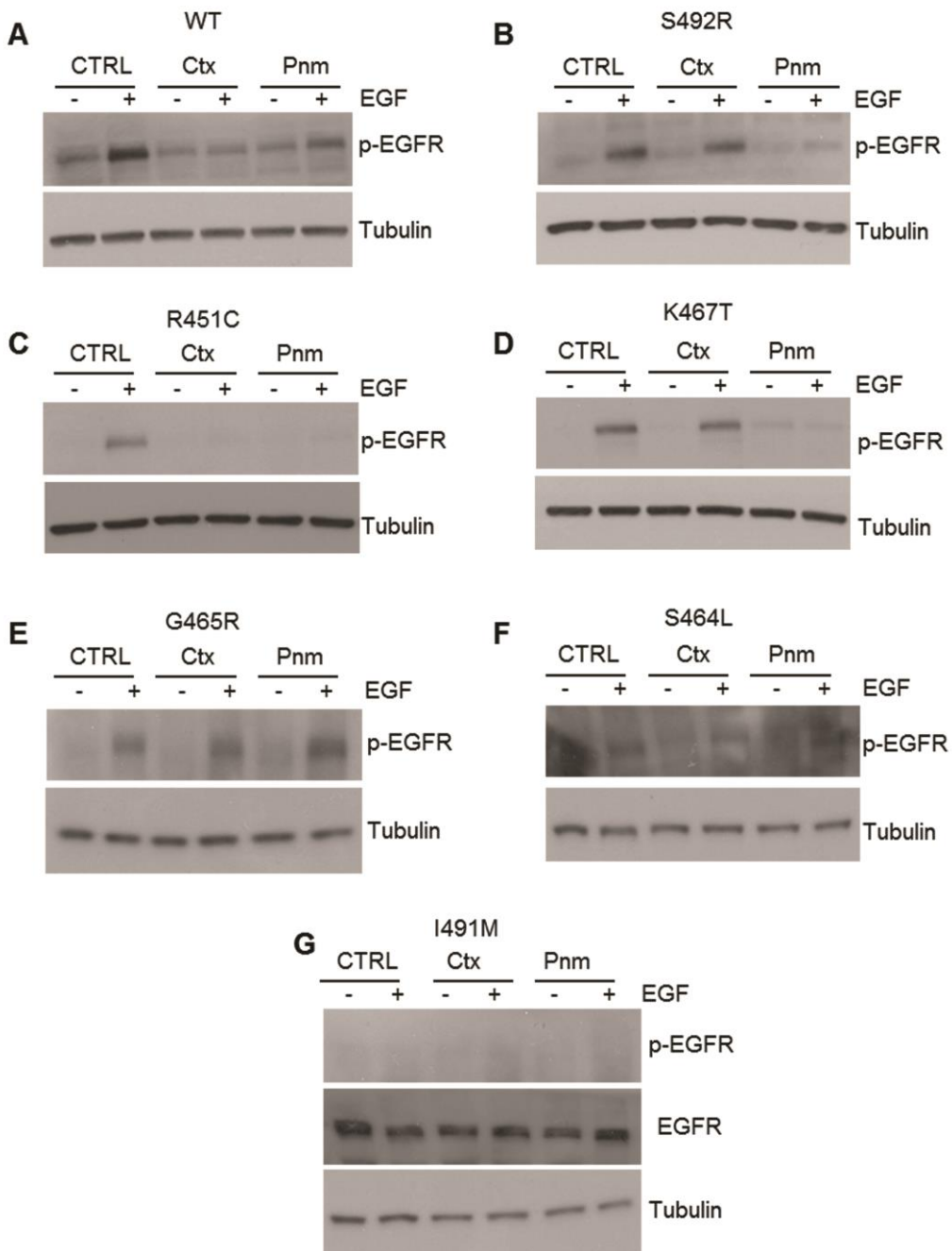
A



B



Arena et al, Figure 3



Supplementary table and figure legends

Supplementary Table S1. Clinical characteristics of patients.

Thirty-seven consecutive metastatic colorectal cancer patients that progressed to cetuximab after an initial response and that had good quality pre- and post- treatment tissue sample were included in this study. Chemotherapy schemes, FOLFOX, oxaliplatin 85 mg m⁻² on day 1, leucovorin 200 mg m⁻² day 1, fluorouracil 400 mg m⁻² bolus day 1, followed by a 2400 mg m⁻² infusion during 22 hours, repeat every 2 weeks; FOLFIRI, irinotecan 180 mg m⁻² on day 1, plus leucovorin 200 mg m⁻², fluorouracil 400 mg m⁻² bolus day 1, followed by a 2400 mg m⁻² infusion during 22 hours, repeat every 2 weeks; cetuximab 400 mg m⁻² initial dose followed by 250 mg m⁻² weekly thereafter; irinotecan 180 mg m⁻² every two weeks; * primary tumor localized in the colon with exact localization non specified.

Supplementary Table S2. Validation of ddPCR probes.

Validation of ddPCR probes on control mutant DNAs to detect EGFR variants previously identified in tumor biopsy or cell.

Supplementary Table S3. Prevalence of EGFR mutations in resistant cell lines.

Prevalence of EGFR mutations in populations of resistant cells analyzed by ddPCR.

Supplementary Figure S1. Nucleotide sequence of the *EGFR* gene in tumor specimen.

Nucleotide sequence (electropherogram) of the *EGFR* gene in tumor specimen from subject 31 and 35 at the time of progression to cetuximab revealing two different heterozygous mutations (K467T and R451C).

Supplementary Figure S2. Comparison of parental and cetuximab resistant cell lines.

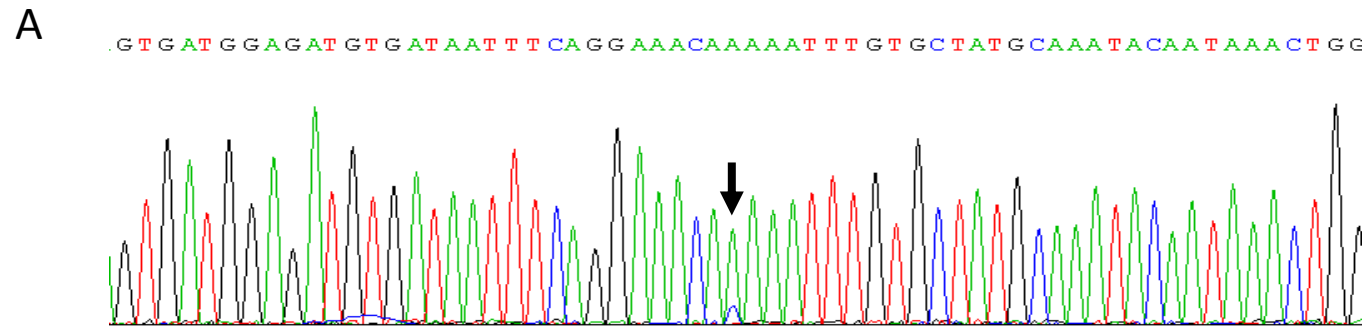
Parental (in red) and cetuximab resistant (in black) DiFi, LIM1215, OXCO-2, HCA-46, NCIH508, and CCK81 cells were treated with increasing concentrations of cetuximab for 1 week. Cell viability was measured by the adenosine triphosphate (ATP) assay. Data points

represent means \pm SD of three independent experiments.

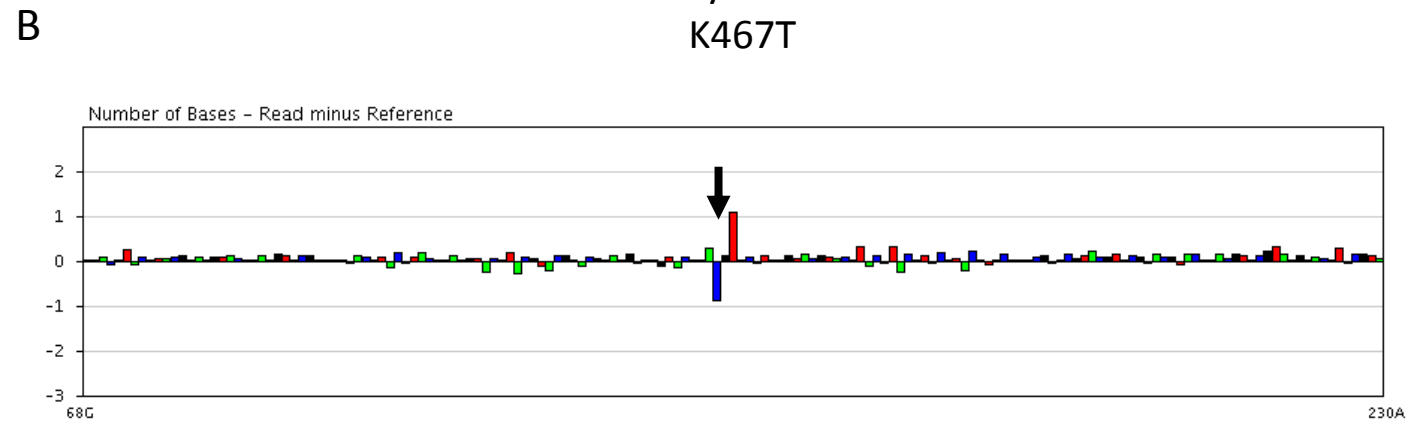
Supplementary Figure S3. Nucleotide sequence of the *EGFR* gene in cetuximab resistant cell lines.

Nucleotide sequence (electropherogram) of the 3 new EGFR variants (S464L, G465R and I491M) found in cetuximab resistant cell lines.

Arena et al, Supplementary Figure S1. Nucleotide sequence of the EGFR gene in tumor specimen.

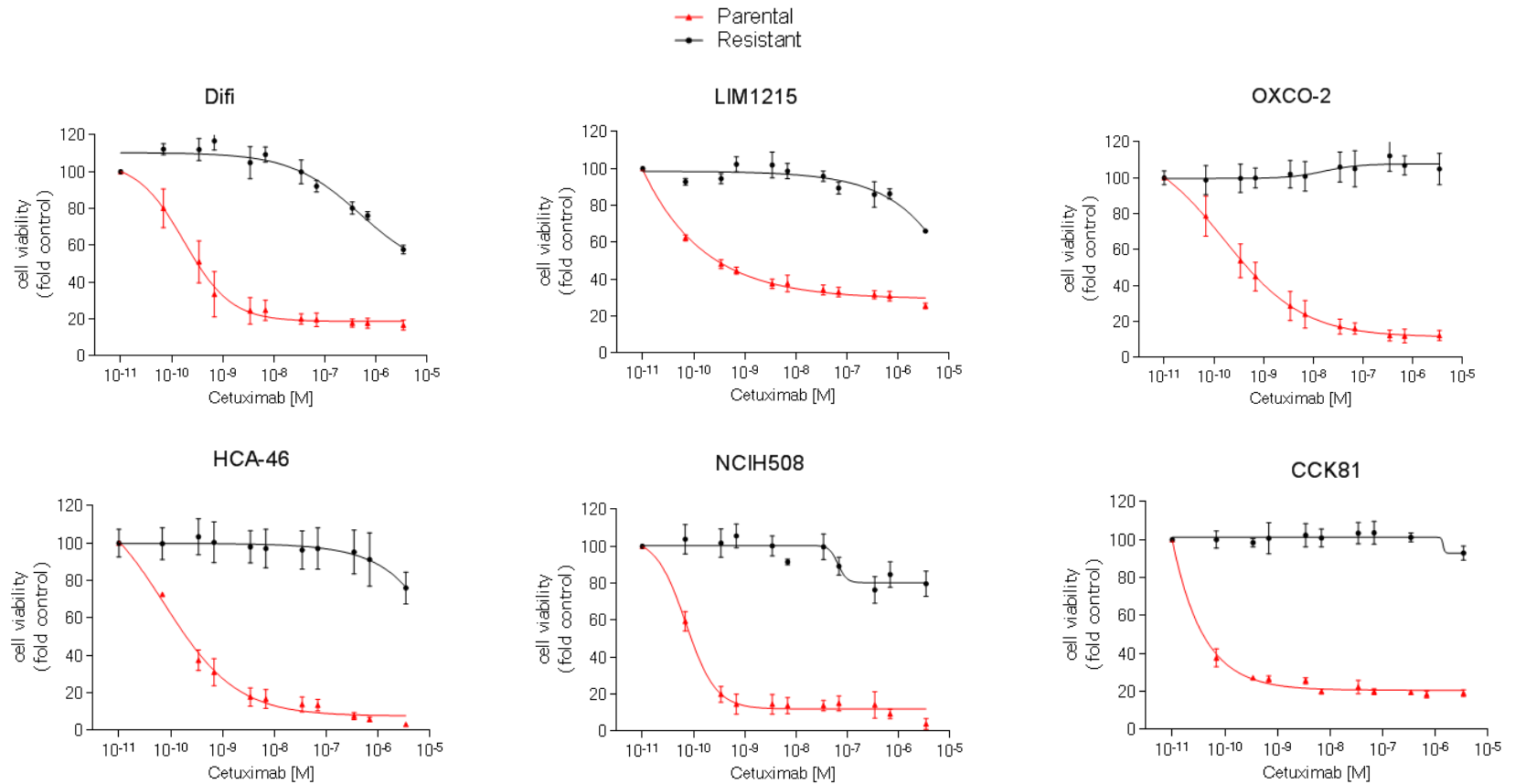


A>C
AAA>ACA
Lys>Thr
K467T

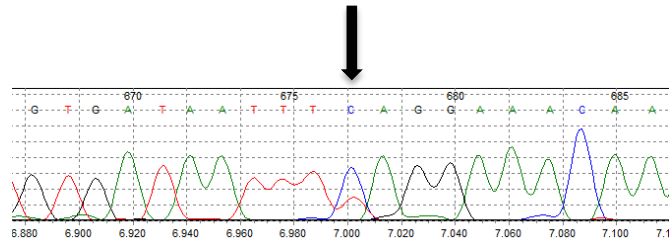


C>T
CGC>TGC
Arg>Cys
R451C

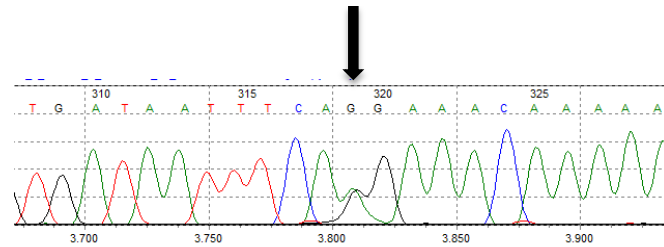
Arena et al, Supplementary Figure S2. Comparison of parental and cetuximab resistant cell lines.



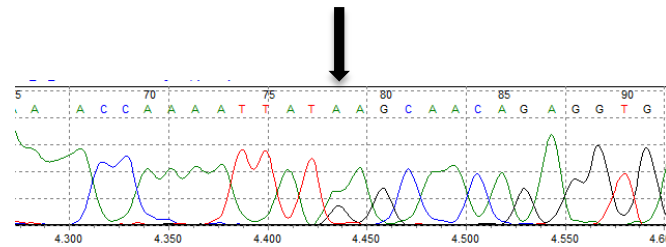
Arena et al, Supplementary Figure S3. Nucleotide sequence of the EGFR gene in cetuximab resistant cell lines.



EGFR S464L 1391C>T



EGFR G465R 1393G>A



EGFR I491M 1473A>G

Arena et al, Supplementary Table S1. Clinical characteristics of patients.

N (total)		37
Age, median (range)		60 (34-80)
Gender, male (%)		25 (67.6)
Primary tumor localization (%)	Caecum	2 (5.4)
	Left colon	0
	Right colon	7 (18.9)
	Sigmoid colon	12 (32.4)
	Rectum	13 (35.1)
	Colon *	3 (8.1)
Stage (%)	III	11 (29.7)
	IV	26 (70.3)
Chemotherapy regimen administered with cetuximab (%)	FOLFOX	9 (24.3)
	FOLFIRI	6 (16.2)
	Irinotecan	20 (54.1)
	Monotherapy	2 (5.4)
Line of cetuximab administration (%)	First	10 (27.0)
	Second	12 (32.4)
	Third	14 (37.8)
	Fourth	1 (2.7)
Radiological response (RECIST)	Stable Disease	22 (59.5)
	Partial Response	14 (37.8)
	Complete Response	1 (2.7)

Arena et al, Supplementary Table S2. Validation of ddPCR probes.

	EGFR p.R451C	EGFR p.S464L	EGFR p.G465R	EGFR p.K467T	EGFR p.I491M	EGFR p.S492R
EGFR 451 plasmid	100%	0,01%	0%	0%	0,02%	0%
EGFR 464 plasmid	0%	100%	0%	0%	0,02%	0%
EGFR 465 plasmid	0,01%	0%	100%	0%	0,01%	0%
EGFR 467 plasmid	0,01%	0%	0,01%	100%	0,01%	0%
EGFR 491 plasmid	0%	0,01%	0%	0%	100%	0%
EGFR 492 plasmid	0%	0,02%	0,01%	0%	0%	100%

Arena et al, Supplementary Table S3. Prevalence of EGFR mutations in resistant cell lines.

Acquired EGFR mutations						
Resistant cell Line	EGFR exon 12					
	R451C	S464L	G465R	K467T	L491M	S492R
CCK81 R1 Cetux		19%				
CCK81 R2 Cetux						
CCK81 R3 Cetux						
DiFi R1 Cetux						
DiFi R2 Cetux						
HCA46 R1 Cetux						
HCA46 R2 Cetux						
LIM1215 R1 Cetux					3.6%	
LIM1215 R2 Cetux						
LIM1215 R3 Cetux						
LIM1215 R4 Cetux						
LIM1215 R5 Cetux			3.1%			
NCIH508 R1 Cetux						
NCIH508 R2 Cetux						
OXCO2 R1 Cetux						
OXCO2 R2 Cetux					3.91%	
OXCO2 R3 Cetux		1.2%				